

Improved Sensitivity for Phosphopeptide Mapping Using Capillary Column HPLC and Microionspray Mass Spectrometry: Comparative Phosphorylation Site Mapping from Gel-Derived Proteins

Francesca Zappacosta,[§] Michael J. Huddleston,[§] Ryan L. Karcher,[†] Vladimir I. Gelfand,[†] Steven A. Carr,^{*,†} and Roland S. Annan^{*}

Department of Computational, Analytical and Structural Sciences, GlaxoSmithKline, King of Prussia, Pennsylvania 19406, and Department of Cell and Structural Biology, University of Illinois at Urbana–Champaign, Urbana, Illinois 61801

Reversible protein phosphorylation regulates many cellular processes. Understanding how phosphorylation controls a given pathway usually involves specific knowledge of which amino acid residues are phosphorylated on a given protein. This is often a nontrivial task. In addition to the difficulties involved in purifying sufficient amounts of any given protein, most phosphoproteins contain multiple, substoichiometric sites of phosphorylation. In this paper, we describe substantial improvements made to our previously reported multidimensional electrospray MS-based phosphopeptide mapping technique that have resulted in a 20-fold increase in sensitivity for the overall process. Chief among these improvements are the incorporation of capillary chromatography and a microionspray source for the mass spectrometer into the first dimension of the analysis. In the first dimension of the process, phosphopeptides present in the proteolytic digest of a protein are selectively detected and collected into fractions during on-line LC/ESMS, which monitors for phosphopeptide specific marker ions. The phosphopeptide containing fractions are then analyzed in the second dimension by either MALDI-PSD or nano-ES with precursor ion scanning. The relative merits and limitations of these two techniques for phosphopeptide detection are demonstrated. The enhancement in sensitivity of the method under the new experimental conditions makes it suitable for phosphorylation mapping (from selective detection through sequencing) on gel-separated phosphoproteins where the level of phosphorylation at any given site is <200 fmol. Furthermore, this method detects serine, threonine, and tyrosine phosphorylation equally well. We have successfully employed this new configuration to map 11 *in vivo* sites of phosphorylation on the *Saccharomyces cerevisiae* protein kinase YAK1. YAK1 peptides containing all five YAK1 PKA consensus sites are phosphory-

lated, suggesting that YAK1 is an *in vivo* substrate for PKA. In addition, four peptides containing cdk sites and the autophosphorylation site at Tyr⁵³⁰ were found to be phosphorylated. Because the first dimension of this method generates a phosphorylation profile that can be used for a semiquantitative evaluation of site specific phosphorylation, we evaluated its ability to detect site-specific changes in the phosphorylation profile of a protein in response to altered cellular conditions. This comparative phosphopeptide mapping strategy allowed us to detect a change in phosphorylation stoichiometry on the motor protein myosin-V in response to treatment with either mitotic or interphase *Xenopus* egg extracts and to identify the single functionally significant phosphorylation site that regulates myosin-V cargo binding.

Reversible protein phosphorylation is arguably the most important mechanism by which signals are transmitted within the cell.¹ Signal transduction through phosphorylation of intracellular proteins plays an essential role in and controls many aspects of cell growth, metabolism, and differentiation. Unraveling the biological pathways leading to these effects often involves understanding how phosphorylation regulates the behavior of individual proteins in the pathway. The first step in this process is usually phosphorylation site mapping of selected pathway components.

Methods for detecting and mapping protein phosphorylation need to be highly sensitive and highly selective. Many regulatory phosphoproteins are expressed in low abundance and are phosphorylated on more than one site, although not all sites are likely to have functional significance. In addition, utilization at any particular phosphorylation site is often substoichiometric. Because regulatory protein phosphorylation is a dynamic process, the stoichiometry at functionally significant sites is likely to change in response to cellular signaling. Thus, in addition to mapping phosphorylation sites, it is equally important to be able to reliably detect changes in phosphorylation stoichiometry. By far the most common approach to identification and quantitation of protein phosphorylation is to isolate the substrate protein from ³²P-labeled cells and to separate tryptic digests of the labeled protein by thin-

* Address correspondence to either author. E-mail: Roland_S_Annan@gsk.com; Carr@mpi.com.

[†] University of Illinois.

[‡] Present address: Millennium Pharmaceuticals, 640 Memorial Drive, Cambridge, MA 02139.

[§] These authors contributed equally to this work.

(1) Hunter, T. *Cell* **1987**, 50, 823–829.

layer chromatography to reveal phosphopeptides. In practice, this is not a trivial exercise, and it is especially unappealing to contemplate the isolation of low-abundance proteins from large cultures of ^{32}P -labeled cells.

Within the last 10 years, mass spectrometry has emerged as a key technology in the difficult task of mapping protein phosphorylation sites.^{2–8} Previously, we described a comprehensive multidimensional phosphopeptide mapping strategy that uses mass spectrometry to isolate and identify phosphorylated peptides.⁵ This strategy takes advantage of the fact that in the mass spectrometer, under experimentally controllable conditions, phosphopeptides undergo facile loss of phosphate from serine, threonine, and tyrosine residues to produce phosphopeptide-specific marker ions at m/z 63 (PO_2^-) and 79 (PO_3^-). In the first dimension of the process, phosphopeptides present in the proteolytic digest of a protein are selectively detected and collected into fractions during on-line LC/ESMS, which monitors for the phosphopeptide specific marker ions at m/z 79 and 63 in the negative ion mode. The inclusion of the chromatographic step results in phosphopeptides' being present in greatly simplified mixtures. In the second dimension of the analysis, the molecular weights of the phosphopeptides in each collected fraction are determined by precursor scans for m/z 79 in the negative ion mode. The high degree of selectivity provided by the precursor scan permits identification of phosphopeptides that are present as very minor components of the fraction. Finally, phosphopeptides are sequenced in the third dimension of analysis by positive ion nanoelectrospray tandem MS of the molecular species identified. The strategy, which has been developed and refined in our laboratory over the past few years, is particularly well-suited to phosphoproteins that are phosphorylated with widely varying stoichiometry at many sites.

The sensitivity of the method as described in our previous work is limited by the HPLC column diameter. Because ESMS (at flow rates above ~ 50 nL/min) acts like a concentration-sensitive detector, smaller internal diameter HPLC columns will provide higher-sensitivity analyses; however the requirement to split the flow postcolumn to allow collection of fractions for subsequent precursor ion scan analysis imposes a practical limitation on the column diameter that can be used. The 0.5-mm-i.d. HPLC columns used in our previous work made it difficult to analyze most SDS-PAGE-derived samples in which the amount of protein available is typically very limited.

We have now significantly improved the sensitivity of this method by incorporating capillary chromatography (0.18-mm i.d.) and a microionspray interface on the mass spectrometer. The microionspray interface incorporates a 7:1 split that allows us to collect $\sim 80\%$ of the sample into fractions. This configuration allows us to detect and identify <200 fmol of phosphopeptides from SDS-PAGE-derived proteins. Because the first dimension of the analysis

utilizes an LC separation coupled to on-line phosphopeptide detection, it generates a phosphopeptide-specific profile of the protein. Here, we illustrate how such a profile can be used to provide a semiquantitative evaluation of how the phosphorylation state of a protein changes under a given set of differing in vivo or in vitro conditions such as growth, development, or compound administration. The comparative profile makes it easier to identify and concentrate analysis efforts on those phosphorylation sites that are relevant to the changing conditions and ignore those that are not.

EXPERIMENTAL SECTION

Protein Samples. The phosphopeptide standards KRPP-SQRHGSKY ($M_r = 1422.7$) and Ac-RRLIEDAEPYAARG-NH₂ ($M_r = 1639.8$) were synthesized at the University of Michigan Protein and Carbohydrate Structure Facility, TRDIYETDYPYRK ($M_r = 1701.7$) was purchased from Anaspec (San Jose, CA), and the two myoglobin tryptic phosphopeptides, LFTGHPEPTLEK ($M_r = 1350.7$) and ApSEDLK ($M_r = 741.4$) were derived from a sample distributed by the Association of Biomolecular Resource Facilities (ABRF) as part of a research study. The ABRF sample consisted of a horse myoglobin tryptic digest, quantitated by AAA and spiked with two synthetic phosphopeptides in a ratio of 1:1 with the nonphosphorylated sequences.⁹

In vivo phosphorylated HA-tagged YAK-1, a 92-kDa protein kinase from *Saccharomyces cerevisiae*, was immunoprecipitated from yeast lysates using anti-HA monoclonal antibody and subsequently applied on a 1-mm one-dimensional gel.¹⁰ The gel was stained with colloidal Coomassie Blue. The band corresponding to YAK-1 was reduced and alkylated and in-gel digested with trypsin.

Purified myosin-V globular tail fragment (MGT) (amino acids 1443–1853) of mouse dilute Myosin Va) was expressed in *Escherichia coli* as a glutathione-(S)-transferase fusion, purified as described and incubated in mitotic or interphase *Xenopus* egg extracts¹¹ in the presence of cold or [γ - ^{32}P]-labeled ATP. After incubation, the GST sequence was removed via cleavage with thrombin, and the MGT was analyzed by SDS-PAGE. Gels were stained with Coomassie Blue and labeled samples were additionally analyzed by autoradiography. Coomassie Blue stained SDS-PAGE bands from MGT incubated in mitotic or interphase egg extracts were excised, reduced, alkylated, and digested with trypsin in situ as described previously.¹²

LC/ESMS. Protein digests were concentrated on an LC Packings (San Francisco, CA) PepMap C18 trap cartridge (300 $\mu\text{m} \times 5$ mm) used in place of the sample loop on the HPLC injector. After washing with 0.1% TFA, the peptides were backflushed off the cartridge at 4 $\mu\text{L}/\text{min}$ using an acetonitrile/water gradient onto an LC-Packings PepMap C18 capillary column, (180 $\mu\text{m} \times 15$ cm, 3- μm particles) fitted directly into the injector. HPLC

(2) Carr, S. A.; Huddleston, M. J.; Annan, R. S. *Anal. Biochem.* **1996**, *239*, 180–192.

(3) Wilm, M.; Neubauer, G.; Mann, M. *Anal. Chem.* **1996**, *68*, 1–8.

(4) Huddleston, M. J.; Annan, R. S.; Bean, M. F.; Carr, S. A. *J. Am. Soc. Mass Spectrom.* **1993**, *4*, 710.

(5) Annan, R. S.; Huddleston, M. J.; Verma, R.; Deshaies, R. J.; Carr, S. A. *Anal. Chem.* **2001**, *73*, 2050–2059.

(6) Posewitz, M. C.; Tempst, P. *Anal. Chem.* **1999**, *71*, 2883–2892.

(7) Nuwaysir, L. M.; Stults, J. T. *J. Am. Soc. Mass Spectrom.* **1993**, *4*, 662–669.

(8) Zhang, X.; Herring, C. J.; Romano, P. R.; Szczepanowska, J.; Brzeska, H.; Hinnebusch, A. G.; Qin, J. *Anal. Chem.* **1998**, *70*, 2050–2059.

(9) Swiderek, K.; Gharahdaghi, F.; Ericsson, L.; Hackett, M.; Fowler, B.; Hathaway, G.; Loo, R. O.; Johnson, R. A.; Stults, J. In *The 1997 ABRF Mass Spectrometry Committee Collaborative Study: Identification of Phosphopeptides in a Tryptic Digest of Apomyoglobin*, ABRF'98: From Genomes to Function—Technical Challenges of the Post-Genome Era, San Diego, CA, 1998.

(10) Kassis, S.; Melhuish, T.; Annan, R. S.; Chen, S. L.; Lee, J. C.; Livi, G. P.; Creasy, C. L. *Biochem. J.* **2000**, *348*, 263–272.

(11) Karcher, R. L.; Roland, J. T.; Zappacosta, F.; Huddleston, M. J.; Annan, R. S.; Carr, S. A.; Gelfand, V. I. *Science* **2001**, *293*, 1317–1320.

(12) Joyal, J. L.; Annan, R. S.; Ho, Y. D.; Huddleston, M. J.; Carr, S. A.; Hart, M. J.; Sacks, D. B. *J. Biol. Chem.* **1997**, *272*, 15419–15425.

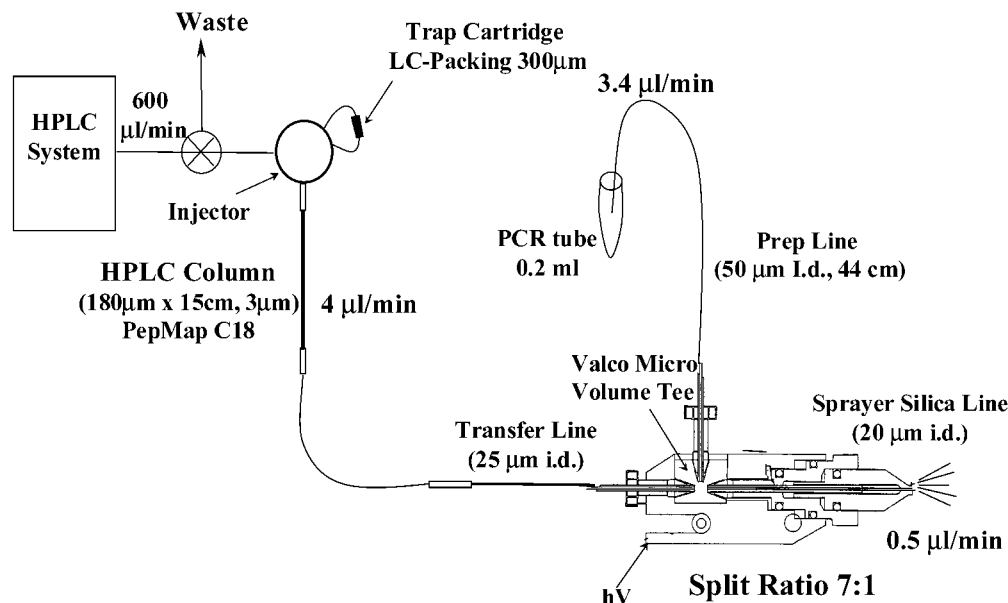


Figure 1. Schematic diagram of the LC/MS system used in this work. The 0.18 mm i.d. HPLC capillary column is fitted directly into the injector. Flow from the HPLC pumps is regulated by a microflow splitter, delivering 4 $\mu\text{L}/\text{min}$ through the column. At the source, the column flow is split $\sim 7:1$, directing 0.5 $\mu\text{L}/\text{min}$ to the MS and 3.5 $\mu\text{L}/\text{min}$ to the prep line for manual collection into PCR tubes.

mobile phases contained either 0.1% formic acid and 0.02% TFA or 0.02% TFA alone. Solvent flow from the HPLC pumps to the injector was regulated by an LC-Packings Acurate microflow splitter. The column outlet was connected to a Micromass nanoflow ion source (Manchester, U.K.) via a 25- μm -i.d. fused-silica line threaded directly into the source (see Figure 1). Column flow was split prior to the MS by means of a 0.15-mm-i.d. micro-volume Valco tee insert (Houston, TX) that directed 0.4–0.6 $\mu\text{L}/\text{min}$ to a 20- μm -i.d. tapered fused-silica electrospray tip from New Objectives (Cambridge, MA). The remainder of the flow was sent to the prep line for manual collection into PCR tubes. The prep line was PEEK (63- μm i.d., 22.5-cm length) from the source tee to a Valco union (SS, 0.15-mm i.d.) and fused silica (50- μm i.d., 45-cm length) on the other side of the union. The prep line union was grounded to prevent electrospray conditions at the exit. MS spectra were recorded on a PE-Sciex API III+ (Concord, Ontario, Canada) triple quadrupole mass spectrometer equipped with a Micromass nanoflow ion source as described above. Negative ion LC/ESMS using single ion monitoring (SIM) for the phosphate specific marker ions m/z 63 (PO_2^-) and 79 (PO_3^-) was performed as previously described.⁴ Fractions were immediately stored at -70°C until needed for further analysis by MALDI/MS or nanospray precursor ion scan.

To reduce the risk of plugging, immediately following LC/ESMS, a syringe was connected in place of the column flow, and methanol was infused to flush the source and split lines free of acetonitrile and TFA. Following this, the syringe was filled with air, and the system was flushed until no liquid was seen coming from the ends of the spray and the prep fused silica.

MALDI Analysis. MALDI mass spectra were recorded on a Micromass ToFSpec SE reflectron time-of-flight mass spectrometer equipped with a time-lag-focusing source. Spectra were calibrated externally using two peptide standards. PSD spectra were recorded in a single segment, and 100–200 laser shots were averaged in a single spectrum. Samples were prepared in α -cyano-4-hydroxycinnamic acid (10 mg/mL in 50/50 ethanol/

acetonitrile). An aliquot of 0.2 μL from each HPLC fraction was mixed with 0.2 μL of matrix solution and 0.2 μL was spotted on the target.

Nanoelectrospray Precursor Ion Scan Analysis. Precursor ion spectra for m/z 79 were recorded on a Sciex API III+ triple quadrupole mass spectrometer equipped with a nanoelectrospray source constructed at the European Molecular Biology Laboratory in Heidelberg, Germany. Typically one-half of each HPLC fraction was taken to dryness and resuspended in 3 μL of 50/50 methanol/water containing 10% ammonium hydroxide (30 wt %), and 1.5 μL was loaded into the nanospray needle for analysis. Spectra were acquired in the MCA mode, as described previously.²

Nano-ES MS/MS Peptide Sequencing. All peptides were sequenced by nanoelectrospray tandem mass spectrometry on a Micromass QTOF. The remaining half of the HPLC fractions was dried and resuspended in 3 μL of either acidic (60/40 methanol/water containing 5% formic acid) or basic (50/50 methanol/water containing 10% ammonium hydroxide) solution. One-half of the sample (1.5 μL) was loaded into the nanospray needle.

RESULTS AND DISCUSSION

Optimization of the Negative Ion Phosphopeptide-Specific LC/ESMS Detection. We previously described a highly selective, multidimensional ESMS-based technique for phosphopeptide mapping.⁵ The procedure uses LC/ESMS in the first dimension to identify phosphopeptide-containing HPLC fractions by monitoring for the presence of phosphate-specific marker ions, m/z 63 and 79. The second dimension employs precursor ion scanning for m/z 79 to determine the molecular weight of the phosphopeptides in the selected fractions.^{2,3} Both of the MS scanning techniques are selective for the phosphate-specific marker ions, thus permitting identification of phosphopeptides in mixtures, even when they are very minor components. Using narrow-bore 0.5-mm-i.d. HPLC columns and a conventional ES source, this system

has an overall sensitivity of 5 pmol of phosphopeptide and has been applied to a variety of phosphoproteins, including calmodulin, which after treatment with the insulin receptor catalytic domain, incorporated two phosphotyrosine residues¹³ and a Net1 mutant that was phosphorylated on serine and threonine residues at over 20 different sites by cdc5 kinase.¹⁴ However, for phosphoproteins that can only be recovered in low amounts, thereby necessitating SDS-PAGE as the final step in purification, we found this sensitivity to be generally insufficient. To detect low stoichiometry phosphorylation sites from in-gel purified proteins, we felt that an increase in sensitivity of at least 10- to 20-fold was needed.

The overall sensitivity of the multidimensional approach described above is limited by the LC separation used in the first dimension of the analysis, not by the MS. It is well-established that UV and ESMS detection sensitivity for peptides separated by LC is a function of analyte concentration in the eluted peaks, as opposed to the absolute amount of sample loaded onto the column. To achieve a high effective peptide concentration in the eluting peaks as absolute sample amounts decrease, it is necessary to use smaller internal diameter columns that maintain high peak separation efficiencies at reduced flow rates of the mobile phase.¹⁵ This has been the driving force for the now routine use of 75- μ m-i.d. RP-HPLC columns for the analysis of femtomole amounts of peptide. However, our strategy requires the phosphopeptides identified by the phosphate-specific LC/ESMS experiment to be collected for further analysis, and it is not practical at present to collect fractions from 75- μ m-i.d. columns during LCMS analysis. Hence, a practical compromise was sought, resulting in the configuration shown in Figure 1. The system uses 0.18-mm-i.d. HPLC columns at a flow through the column of 4 μ L/min. The outlet of the column is connected to the nanoflow ionspray source via a 25- μ m-i.d. fused-silica transfer line. The column flow is split (\sim 7:1) at the source, directing 0.5 μ L/min to the ES tip and 3.5 μ L/min to the prep line for manual collection into PCR tubes.

To further improve the sensitivity of the negative ion LC/ESMS system, we switched from 0.1 to 0.02% TFA as acid modifier in the HPLC mobile phases. However, during the course of these studies, we found that the low acid strength of the reduced TFA mobile phase had a deleterious effect on the peak shape and recovery of late eluting, low abundance hydrophobic peptides (data not shown). To improve the ion-pairing strength of the mobile phase, we added 0.1% formic acid to the 0.02% TFA-containing solvent. The inclusion of the 0.1% formic acid to the 0.02% TFA in the HPLC mobile phase significantly improved chromatographic peak shape such that we observed a 2–3-fold increase in sensitivity over 0.02% TFA alone (data not shown). The use of the described new instrument configuration and the modified HPLC mobile phase yielded a gain in LC/ESMS detection sensitivity of 20–40-fold while still allowing fraction collection of phosphopeptides.

To test the ultimate sensitivity of our reconfigured LC/ESMS system, we used a mixture of five synthetic peptides, (1) KRPPSQRHGSKY (M_r = 1422.7), (2) TRDIYETDYPYRK (M_r = 1701.7), (3) LFTGHPEPTLEK (M_r = 1350.6), (4) Ac-RRLIED-

AEpYAARG-NH2 (M_r = 1639.8) and (5) ApSEDLK (M_r = 741.3), spiked in equimolar amounts into an equivalent amount of horse apomyoglobin tryptic digest. This sample represents a protein with quantitative phosphorylation at 5 sites. The mixture was analyzed by negative ion LC/ESMS-SIM for m/z 63 and 79. At levels of 500 and 250 fmol injected, four of the five peptides were readily detected with good S/N (Figure 2A). Peptide 5, ApSEDLK (M_r = 741.3), was not recovered at any level injected. Because of its low molecular weight and hydrophilic nature, it is unretained and elutes in the column void. The loss of this phosphopeptide highlights one of the limitations of a phosphorylation mapping method that used reversed-phase chromatography. At 125 fmol injected, the first three eluting peptides, KRPPSQRHGSKY (1), TRDIYETDYPYRK (2), LFTGHPEPTLEK (3) were still detected with good S/N, but the more hydrophobic peptide, Ac-RRLIEDAEpYAARG-NH2 (4), which elutes last, was no longer detectable. These analyses suggest that the working sensitivity of the LC/ESMS system for phosphopeptide detection and fractionation is between 100 and 200 fmol.

Because only a small percentage of the HPLC eluent is necessary for MS analysis, \sim 5/6 of the sample (\sim 3–4 μ L) can be diverted and manually collected into PCR tubes to be used for further analysis. Each of the individual phosphopeptide peaks from the 500, 250, and 125 fmol samples described above were manually collected and analyzed by two different MS approaches to identify the phosphopeptides in each of the selected fractions. Fractions were analyzed by MALDI-PSD to detect the loss of phosphate from peptide precursor ions¹⁶ and nanoelectrospray using precursor ion scanning for m/z 79. The limited amount of sample available in each fraction, both in terms of amount and volume (\sim 3 μ L), allowed us to assess the sensitivity and strengths and weaknesses of these two methodologies.

In the flight tube of a MALDI-TOF mass spectrometer, phosphopeptides readily undergo metastable decomposition to produce abundant $[MH - H_3PO_4]^+$ and $[MH - HPO_3]^+$ ions.¹⁶ In a reflectron instrument, these fragment ions can be properly focused and detected at their correct masses using a single step post source decay¹⁷ experiment. We have shown previously that by using sufficiently high laser energies, this experiment has a sensitivity on the order of 20 fmol.¹⁸ Because of the high sensitivity and the ease and speed of doing MALDI experiments, we decided to revisit this approach to phosphopeptide identification. In addition, we felt that it might represent a possible alternative for laboratories not equipped with a triple quadrupole instrument to perform precursor ion scans for phosphopeptide detection.

A 0.2- μ L aliquot of each fraction (\sim 1/20 of the total fraction) was analyzed by MALDI and MALDI-PSD. By way of example, we show here data collected from fractions 1 and 3 of the 250-fmol sample. Figure 2B shows the presence of a single peptide at MH^+ 1423.8 in fraction 1. The PSD spectrum for this precursor (Figure 2B, inset) shows the loss of 98 Da, typical of serine and threonine phosphopeptides.¹⁶ The MALDI spectrum of fraction 3 shows two major peaks at 1271.8 and 1351.8 Da (Figure 2C). PSD of each showed that only the 1351.8 ion could generate an MH^+ –

(13) Annan, R. S.; Carr, S. A. *J. Protein Chem.* **1997**, *16*, 391–402.

(14) Chen, S. L.; Huddleston, M. J.; Carr, S. A.; Annan, R. S.; Shou, W.; Deshaies, R. J. Proceedings of the 48th Conference on Mass Spectrometry and Allied Topics, Long Beach, CA, 2000.

(15) Simpson, R. J.; Moritz, R. L.; Begg, G. S.; Rubira, M. R.; Nice, E. C. *Anal. Biochem.* **1989**, *177*, 221–236.

(16) Annan, R. S.; Carr, S. A. *Anal. Chem.* **1996**, *68*, 3413–3421.

(17) Kaufmann, R.; Spengler, B.; Lutzenkirchen, F. *Rapid Commun. Mass Spectrom.* **1993**, *7*, 902–910.

(18) Chen, S. L.; Annan, R. S.; Carr, S. A. Proceedings of the 47th Conference on Mass Spectrometry and Allied Topics, Dallas, TX, 1999.

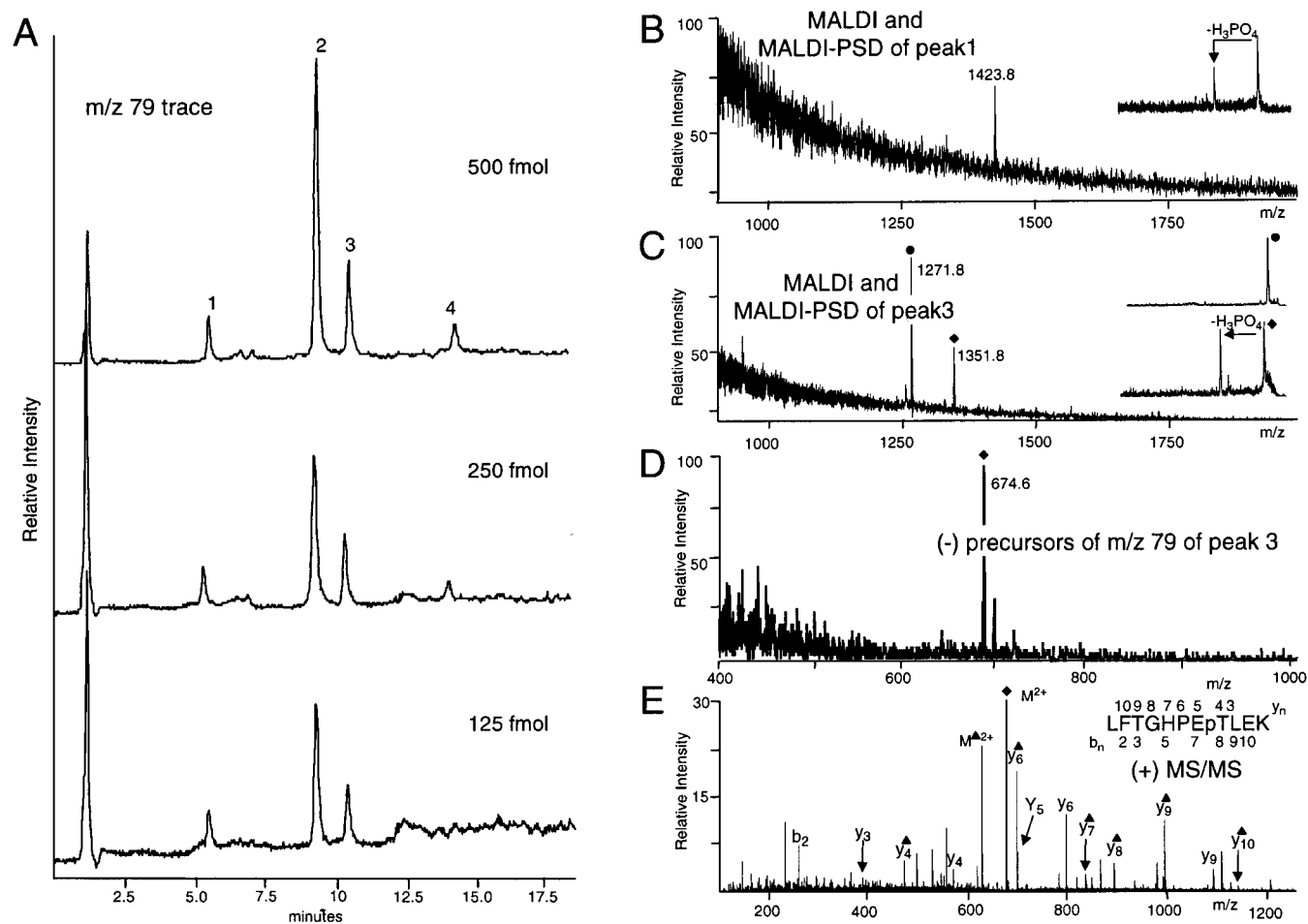


Figure 2. Phosphorylation mapping sensitivity using capillary column LC and microionspray MS. An equimolar mixture of five phosphopeptides (see text for peptide sequences) spiked into an equivalent amount of horse apomyoglobin tryptic digest was analyzed using the reconfigured LC/MS system described in Figure 1. (A) Negative ion LC/ESMS trace for m/z 63 and m/z 79 (summed) using decreasing amounts of sample (500, 250, and 125 fmol). A blank was injected between each run. Peptide 5 (ApSEDLK) eluted in the column void and was not recovered. Fractions containing peaks were subjected to further analysis. (B) Identification of phosphopeptide(s) in fraction 1 by MALDI-PSD. An aliquot ($\sim 1/20$) of the phosphopeptide containing the fraction from the 250-fmol sample was analyzed by MALDI and MALDI-PSD. A single peptide at $MH^+ 1423.8$ was detected in the MALDI spectra. PSD spectrum of the 1423.8 ion shows the presence of the $[MH - 98]^+$ ion typical of serine and threonine phosphopeptides (inset). (C) Identification of phosphopeptide(s) in fraction 3 by MALDI-PSD analysis. About 1/20 of fraction 3 from the 250 fmol sample was analyzed by MALDI and MALDI-PSD. The MALDI spectrum shows two peptides, $MH^+ 1271.8$ and 1351.8, but PSD analysis showed that only the 1351.8 ion fragments produced the $[MH - 98]^+$ ion (insets). (D) Identification of phosphopeptides by $(-)$ ion nano-ES showing the selectivity of the precursor ion scan. One-half of fraction 3 described above was analyzed by a negative ion precursor ion scan monitoring for the phosphopeptide marker ion at m/z 79. A single phosphopeptide with average mass of 1351.2 was detected. The satellite peaks correspond to Na^+ adducts. (E) Determination of the phosphorylation site of the phosphopeptide in fraction 3. The remaining one-half of fraction 3 from above was analyzed by positive nano-ES MS/MS on a QTOF instrument. The y_n ion series allowed the determination of the phosphorylation site. For the sake of clarity, not all ions are labeled. The actual sequence coverage is indicated on the peptide sequence. Peptide fragment ion nomenclature is that of Biemann,²⁹ except that b_n^+ or y_n^+ refers to $[b_n - H_3PO_4]^+$ and $[y_n - H_3PO_4]^+$ and M^{2+} and M^{2+} refer to $[M + 2H]^{2+}$ and $[M + 2H - H_3PO_4]^{2+}$, respectively.

98 fragment ion (Figure 2C, insets). The peptide at $MH^+ 1351.8$ is, in fact, the phosphorylated peptide LFTGHPEpTLEK, and the peptide at $MH^+ 1271.8$ is the nonphosphorylated analogue, which was recovered in the same fraction.

As the complexity of the HPLC fraction increases, the MALDI-PSD confirmation of phosphopeptides becomes more challenging, since there is no way a priori to select phosphopeptides for PSD analysis. Two obvious selection criteria are to perform PSD on all the major peaks and to perform PSD on any peptides that cannot be assigned to a predicted tryptic peptide. Unfortunately, phosphopeptides generally seem to ionize less efficiently than nonphosphorylated peptides and, thus, tend to be minor components of most mixtures. In these cases, a longer gradient to

improve the LC separation might sufficiently simplify the peptide mixture to make MALDI-PSD a viable alternative.

A more selective way to identify phosphopeptides in mixtures is through the use of a precursor ion scan for the phosphate marker ion, m/z 79. Each fraction described above was taken to dryness and resuspended in a basic solution, and one-half of it was analyzed by nano-ES using a precursor ion scan. In each fraction of the 250- and 500-fmol samples, we identified a single phosphopeptide with a signal-to-noise $>10:1$ (for example, see Figure 2D). Although these data suggested that the sensitivity limit of the method had not been reached, we were not able to identify any phosphopeptides in the 125-fmol sample. Considering the sensitivity of the MS response shown in Figure 2D, it is likely

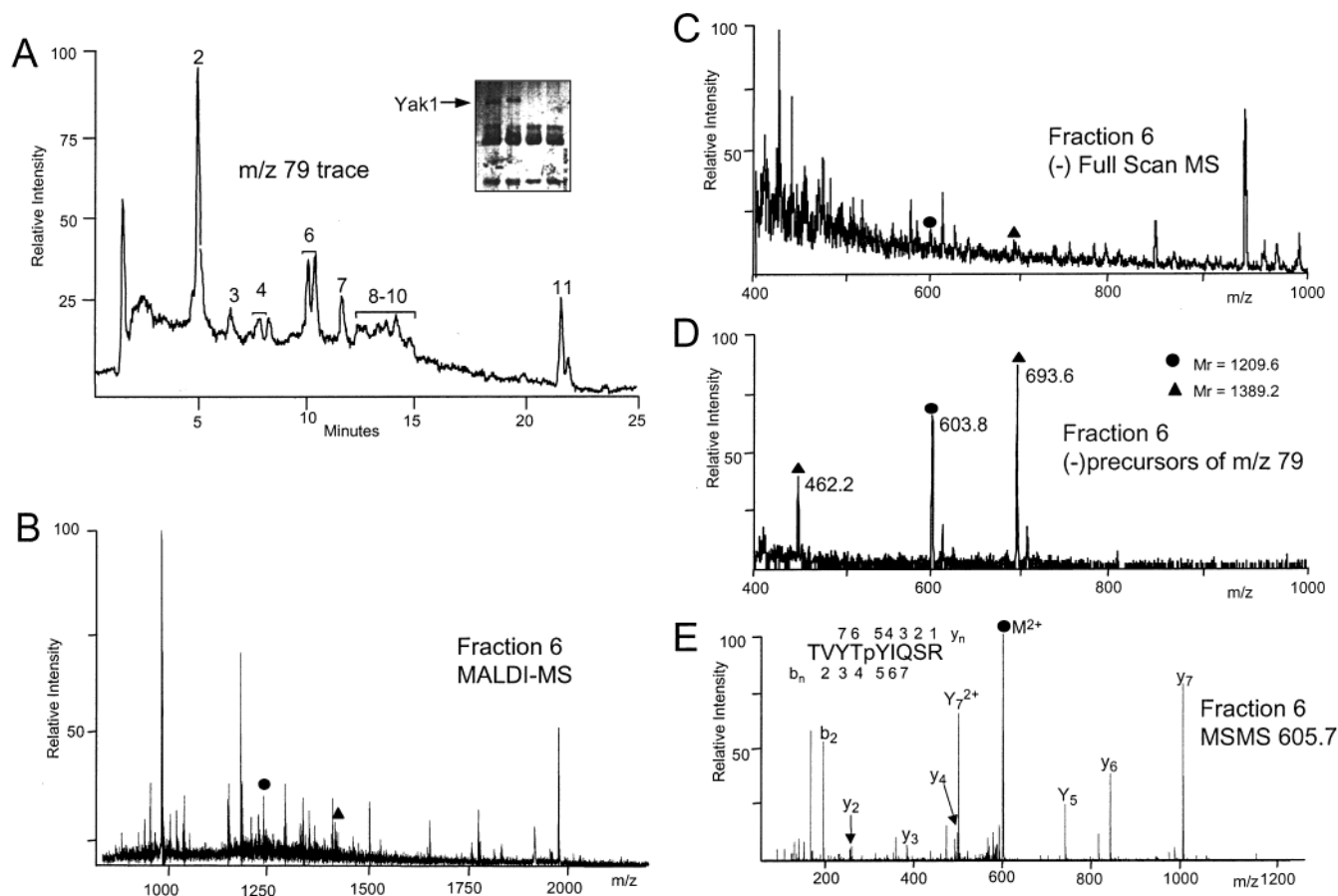


Figure 3. Phosphopeptide mapping of in vivo derived YAK1 from *S. cerevisiae*. YAK1 was immunoprecipitated from yeast whole cell lysates and purified by SDS-PAGE. The Coomassie-stained YAK1 band (marked with an arrow in part A, inset) was in-gel digested with trypsin, and the peptide mixture was analyzed by LC/MS as described in the text. The sample was spiked with 500 fmol of KRPpSQRHGSKY as an internal standard (peak 2). (A) LC/ESMS trace for m/z 79 and 63. Fractions were manually collected for further analysis. (B) MALDI spectrum of fraction 6. The complexity of the fraction made it impossible to select peptides for analysis by PSD. Peaks marked were later identified by precursor ion scanning as phosphopeptides. (C) Nano-ES full-scan (–) ion MS spectrum from fraction 6. (D) Nano-ES (–) ion m/z 79 precursor scan of fraction 6. The spectrum shows doubly and triply charged ions for two phosphopeptides with average masses of 1209.6 and 1389.2. (E) Nano-ES (+) ion CID product ion spectrum of the doubly charged ion (m/z 605.7) for the 1209.6 peptide found in fraction 6. The y_n ion series identifies this peptide as residues 526–534 + P and unambiguously determines the site of phosphorylation as Tyr⁵³⁰.

that this failure was due to sample handling and peptide storage following the HPLC fractionation. We have learned that when working with low abundance phosphopeptides, it is imperative to carry out the whole phosphorylation mapping procedure in the shortest time possible, never letting the fractions sit for more than a day or two.

Once the phosphopeptides in each fraction have been identified, using either of the methodologies discussed above, the sequence of the phosphopeptide is verified, and the specific site of phosphorylation is determined using nano-ES tandem MS (MS/MS) in the positive ion mode. In our experience, some phosphopeptides (KRPpSQRHGSKY, for example) have a better positive ion MS response in a basic solution, so the sample remaining from the precursor scan analysis is generally used for the initial attempt at sequencing. If this proves refractory, then the remaining sample is acidified with formic acid and used for sequencing. Figure 2E shows the positive ion MS/MS spectra of the doubly charged phosphopeptide LFTGHPEpTLEK at m/z 676.2 isolated in fractions 3 from the 250-fmol sample and sequenced in acidic conditions. The exact phosphorylation sites can be determined by the y_n series.

Phosphorylation Mapping of SDS-PAGE Derived Proteins. To demonstrate the ability of the multidimensional ESMS based method to map multiple substoichiometric phosphorylation sites on an SDS-PAGE-derived protein, we mapped the in vivo phosphorylation sites on the *S. cerevisiae* protein kinase Yak1. Yak1 is a 92 kDa novel dual function protein kinase that autophosphorylates on tyrosine residues and can phosphorylate other proteins on serine and threonine residues.^{19,10} In yeast, Yak1 is an antagonist of the Ras/cAMP-dependent protein kinase pathway, acting as a negative regulator of cell growth. Yak1 homologues that have been identified are mammalian DYRK1, DYRK2, DYRK3, *Drosophila* minibrain, *Schizosaccharomyces pombe* Z50142 and *Caenorhabditis elegans* Z70308. Yeast Yak1 is extensively phosphorylated in vivo by other protein kinases¹⁹ and maintains some level of phosphorylation on the autocatalytic Tyr⁵³⁰ residue.

Yak1 was purified from yeast cell lysate by immunoprecipitation and separated on a 1D-gel (Figure 3A, inset). A single Coomassie Blue-stained band corresponding to ~200 ng of protein (~2.0

(19) Garrett, S.; Menold, M. M.; Broach, J. R. *Mol. Cell Biol.* **1991**, *11*, 4045–4052.

Table 1. In Vivo Phosphorylation of SDS-PAGE Derived Yak1

HPLC fraction	M_r found ^a	residues	M_r calc	sequence ^b
2	854.8	293–299 + 1HPO ₃	854.8	(R)RASLNSK
4	1525.2	124–135 + 2HPO ₃	1525.6	RRKSSSLVVPPAR
	1369.2	125–135 + 2HPO ₃	1369.4	(R)RKSSSLVVPPAR
	1288.8	125–135 + 1HPO ₃	1289.4	(R)RKSSSLVVPPAR
	1132.8	126–135 + 1HPO ₃	1133.2	(RR)KSSSLVVPPAR
6	1389.2	279–290 + 1HPO ₃	1389.4	NDLQPVLNATPK
	1209.6	526–534 + 1HPO ₃	1210.2	TVYTYIQSR
7	1123.6	300–309 + 1HPO ₃	1124.2	TLSPVSVTK
8–10	2223.0	238–255 + 3HPO ₃	2223.2	(R)RLSAYPPSTSPPLQPPFK
	2142.6	238–255 + 2HPO ₃	2143.2	(R)RLSAYPPSTSPPLQPPFK
	1750.4	191–203 + 1HPO ₃	1750.8	(R)FVPSLYDRQDFQR
	3646.2	205–237 + 1HPO ₃ + Mox	3647.9	(RR)QSLAATNYSSNFSSL- NSNTNQGTNSIPVMSPYR

^a All values are reported as average mass. ^b Amino acid sequence of phosphorylated tryptic peptides. Relevant amino acids upstream of the N-terminal residue are shown in parentheses. Underlined sequences represent PKA consensus motifs ([R,K]₂-X-[S,T]). Italicized sequences represent Cdk consensus motifs [S,T]-P. Ser, Thr and Tyr residues that are in kinase consensus sequences or have been shown by direct sequencing to be phosphorylated are shown in boldface.

pmol) was digested with trypsin and one-half of the sample fractionated using the phosphate-specific LC/ESMS system (Figure 3A). The sample was spiked with 500 fmol of internal standard KRPPSQRHGSKY (fraction 2) prior to injection. Phosphopeptide-containing peaks were manually collected and further analyzed. On the basis of the intensity of the internal standard peak, we estimate that ~200 fmol or less of each phosphopeptide was present in the sample injected. Each fraction was first analyzed by MALDI-PSD using ~1/15 of the fraction. Unfortunately, we were not able to identify any phosphopeptide. Figure 3B shows the extreme complexity of the MALDI spectrum for fraction 6. The large number of peaks present in the fraction made it impossible to intelligently select peaks for PSD analysis.

In light of the failure of the MALDI analysis to detect any phosphopeptides, an aliquot of each fraction was, therefore, made basic and analyzed by negative ion precursor scanning for m/z 79. The precursor scan for fraction 6 is shown in Figure 3D. Three major signals that correspond to two phosphopeptides (M_r = 1389.2 and 1209.6 Da) are detected. The corresponding full-scan negative ion ESMS spectrum (Figure 3C), along with the MALDI spectrum (Figure 3B), shows that both phosphopeptides are minor components of the fraction. These data support the presumption of low-phosphorylation stoichiometry on the basis of the response of the phosphopeptides relative to the amount of protein digest injected. The superiority of the precursor ion scan for selectively detecting low abundance phosphopeptides in the presence of a large amount of non phosphorylated peptides is clearly demonstrated.

On the basis of the molecular weights, we could assign these phosphopeptide signals to Yak1 sequences 279–290 (NDLQPV-LNATPK) and 526–534 (TVYTYIQSR), each containing a single mole of phosphate. The remaining sample in basic solution was used to localize the site of phosphorylation for both peptides by nano-ES MS/MS. A product ion spectrum for the doubly charged ion, m/z 605.7, from the 526–534 + P peptide is shown in Figure 3E. The phosphorylation site was determined from the y_n series to be the previously described autophosphorylation site Tyr^{530,10}

All of the Yak1 fractions were analyzed by precursor ion scanning for m/z 79. In total, we identified 12 phosphopeptides

corresponding to at least 11 phosphorylation sites (Table 1). Two of the fractions (3 and 11) did not yield any data. In *S. cerevisiae*, Yak1 expression is regulated by the cyclic AMP-dependent protein kinase (PKA) through a transcriptional activator, Msn2.²⁰ It has been suggested that Yak1 is also a substrate for PKA, and indeed, Yak1 can be phosphorylated by PKA in vitro. Data suggesting that Yak1 is an in vivo substrate for PKA are ambiguous, though Garret¹⁹ has demonstrated clearly that if Yak1 is phosphorylated by PKA in the cell, it is also a substrate for at least one other kinase, as well.

Phosphopeptides containing all five YAK1–PKA consensus sites were identified in our analysis (Table 1), suggesting that Yak1 is, indeed, an in vivo substrate for PKA. In addition, we identified four phosphopeptides that contained cyclin-dependent kinase (cdk) motifs. Cdk phosphorylation sites on Yak1 are consistent with Yak1's proposed role in the cell cycle.¹⁹ Finally, there were two other phosphopeptides that did not contain any identifiable consensus motif.

The identification of 11 unique phosphorylation sites on Yak1 from a single gel slice demonstrates that the sensitivity of this method is suitable for the analysis of gel-derived phosphoproteins in which the level of phosphorylation is between 100 and 200 fmol. It is capable of detecting phosphorylation on serine, threonine, and tyrosine equally well at these levels. Furthermore, the example of Yak1 shows that the sensitivity and selectivity of the multidimensional ESMS approach allow detection of phosphopeptides from gel-derived proteins, even when the stoichiometry is quite low. Nonspecific detection methods, such as MALDI, failed in this case both because of the complexity of the peptide mixture and because of the weak intensity of the phosphopeptide signals.

Comparative Phosphopeptide Mapping from Gel-Derived Proteins. As the signal that switches on and off biological pathways, protein phosphorylation changes in response to extracellular stimuli or intracellular events. Thus, monitoring the level of phosphorylation at specific sites provides very valuable insights into the mechanism by which these pathways are regulated. Because the first dimension of the method described here uses LC/ESMS as the readout for the phosphorylation state of a

(20) Smith, A.; Ward, M. P.; Garrett, S. *EMBO J.* **1998**, *17*, 3556–3564.

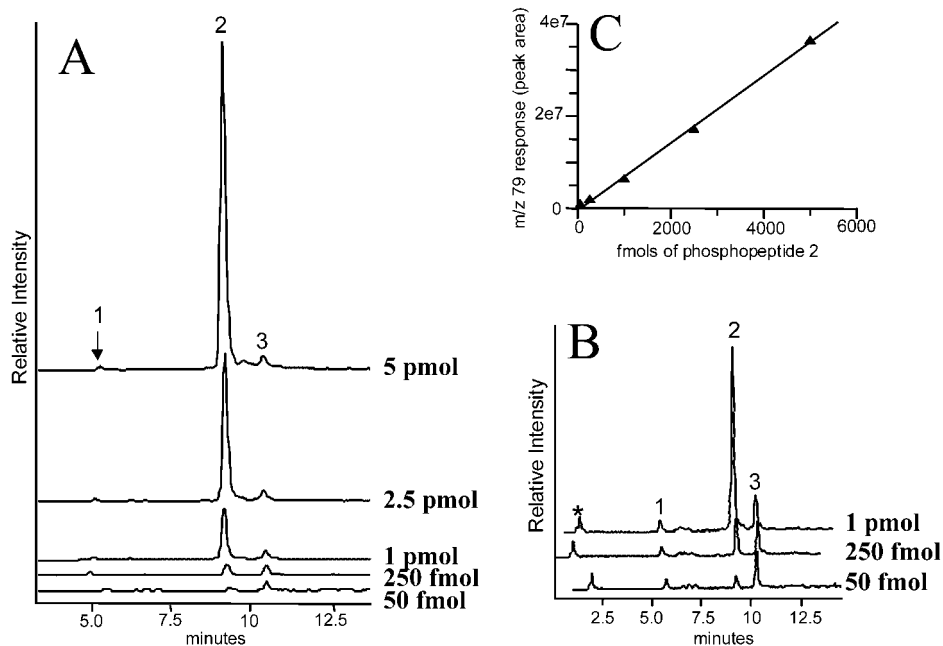


Figure 4. Phosphopeptide-selective LC/MS monitoring of site-specific changes in phosphorylation profile. (A) LC/ESMS traces for m/z 79 and 63 for phosphopeptides 1–3. Phosphopeptides 1 and 3 were kept constant (0.5 pmol), while phosphopeptide 2 was varied (0.05–5.0 pmol). (B) Enlarged view of the LC/ESMS traces corresponding to the three lower peptide concentrations. Peak marked with an asterisk corresponds to the injection peak. (C) Linearity of MS response for m/z 79 with changing phosphopeptide amount. At low peptide concentration, the MS response was not completely linear; however, variation in response for a single phosphopeptide could be reliably detected over a range of 100-fold.

protein, it should be able to generate reproducible phosphorylation profiles equivalent to a 2D-phosphopeptide map, but in a much shorter time and without the radioactivity. Furthermore, it could be used to study the change in phosphorylation state of a protein in response to cellular changes. To validate if the LC/ESMS-SIM approach could be used to evaluate changes in phosphorylation stoichiometry, we analyzed a mixture of three phosphopeptides, (1) KRPPSQRHGSKY, (2) TRDIYETDYPYRK, and (3) LFTGH-PEpTLEK, keeping the amounts of 1 and 3 constant (0.5 pmol), while varying the amount of peptide 2 from 0.050 pmol to 5.0 pmol. Figure 4 shows that a relative change in the amount of phosphopeptide present in a sample could be reliably detected, using the m/z 79 ion current trace, over a range of 100-fold. The response for peptide 2, however, is not completely linear at lower concentration; therefore, the approach should not be considered strictly quantitative.

We tested the ability of this method to detect relative changes in phosphorylation stoichiometry by analyzing the phosphorylation profiles of myosin-V tail fragment (MGT) treated with either mitotic or interphase *Xenopus* egg extracts. Myosin V is a motor protein involved in the transport of organelles along actin-based filaments.²¹ During mitosis, organelle transport shuts down so that it does not interfere with the cell-division machinery. It has been recently shown that myosin-V binding of organelles is cell-cycle-dependent and that it may be regulated by phosphorylation of the cargo-binding tail.²² Figure 5A (inset) shows that mitotic (M) but not interphase (I) extracts of *Xenopus* egg phosphorylate the 48 kDa MGT. To elucidate the mechanism by which myosin-V-driven organelle transport is cell-cycle-regulated, we compared the phosphorylation profiles of the samples and mapped the

phosphorylation sites. Coomassie-stained bands corresponding to both mitotic and interphase treated MGT were excised and digested with trypsin. One-half of each sample was analyzed for phosphopeptide content using the first dimension capillary LC/ESMS method described here. Figure 5A shows one major (fraction 8) and two minor (fractions 7 and 9) phosphopeptide-containing peaks in the mitotic MGT sample (Figure 5A, open line trace), which are not present in the interphase MGT sample (Figure 5A, shaded trace). Fractions 7–9 were collected manually and analyzed by MALDI-PSD and nano-ES with precursor ion scans for m/z 79 (see below). The other phosphopeptides present in both mitotic and interphase samples (e.g., peaks between 3.7 and 11 min. and ~31 min.) arise from basal *in vivo* phosphorylation. Phosphorylation at these sites is apparently at very low stoichiometry, as indicated by the trace amounts of ³²P incorporated at interphase (gel in Figure 5A). The reproducibility of the m/z 79 trace in terms of peak heights and relative ratios of these other phosphopeptide-containing peaks in the interphase and mitotic samples is worth noting (Figure 5A).

Using ~1/15 of each fraction, MALDI-PSD was performed on ion signals that could not easily be assigned to MGT tryptic peptides. Figure 5B shows the MALDI spectrum for fraction 8. PSD was performed on all of the marked signals. Only the ion at MH^+ 1921.9 showed the diagnostic loss of phosphate (inset, Figure 5B). Both fractions 7 and 9 also showed the presence of an ion at MH^+ 1921.9 that could lose phosphate. This peptide could be assigned to myosin-V residues 1648–1664 (TSSIADE-GTYTLDSILR) plus one mole of phosphate. To define the location of the phosphorylation site(s) among the 7 potential phosphorylation sites, we sequenced the 1921 Da peptide in all three fractions

(21) Reck-Peterson, S. L.; Provance, D. W., Jr.; Mooseker, M. S.; Mercer, J. A. *Biochim. Biophys. Acta* **2000**, *1496* (1), 36–51.

(22) Rogers, S. L.; Karcher, R. L.; Roland, J. T.; Minin, A. A.; Steffen, W.; Gelfand, V. I. *J. Cell Biol.* **1999**, *146*, 1265–1276.

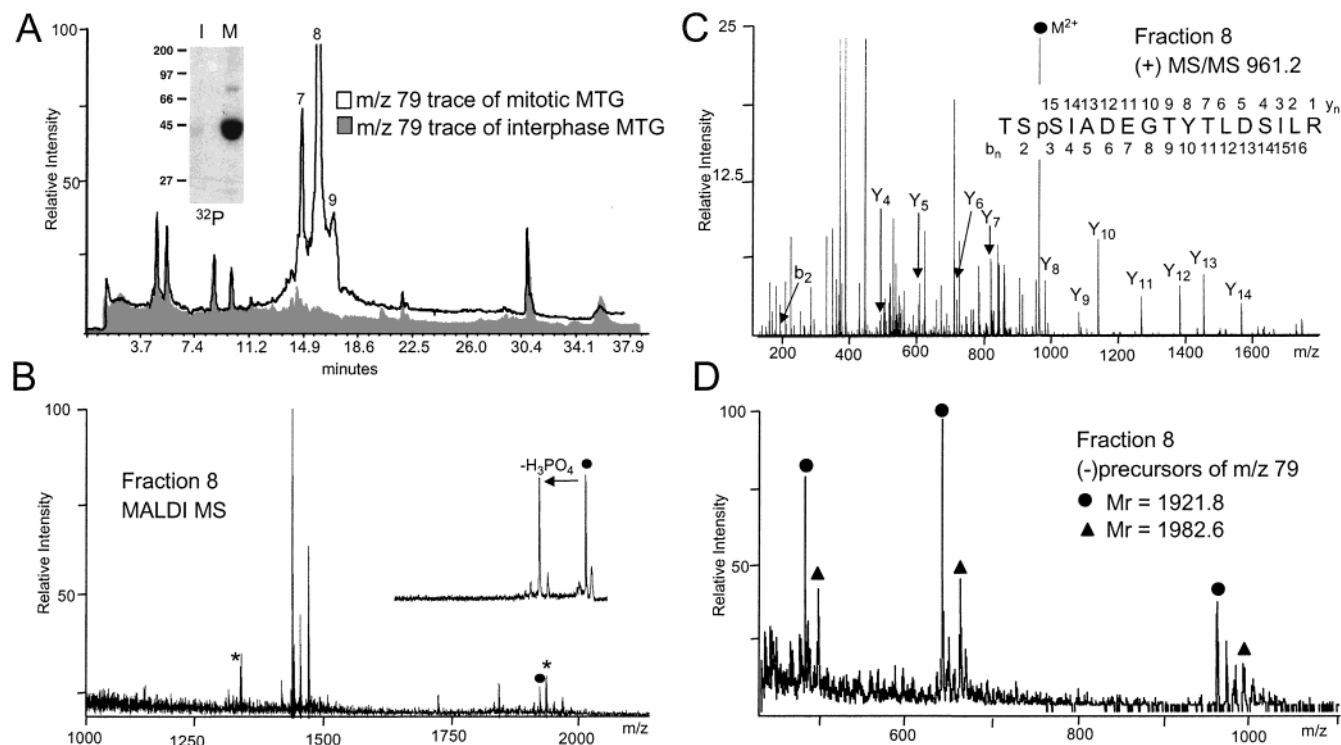


Figure 5. Comparative phosphopeptide mapping of myosin-V (MTG). Mitotic (M) but not interphase (I) extracts from *Xenopus* egg phosphorylates MTG (A, inset). Coomassie-stained bands corresponding to both mitotic and interphase MTG were digested with trypsin and analyzed by LC/MS, as described in the text. (A) LC/ESMS traces for m/z 79 and 63. The trace for the mitotic sample (white) is compared with the trace for the interphase sample (gray). Three major phosphopeptide-containing fractions were detected in the mitotic sample. (B) MALDI and MALDI-PSD spectra of fraction 8. PSD was performed on those ions that could not easily be assigned to any MTG tryptic peptide (marked with symbols). Only the ion at $MH^+ - 98$ showed the $MH^+ - 98$ loss typical of serine and threonine phosphopeptides (inset). (C) Nano-ES (+) CID product ion spectrum of doubly charged ion (m/z 961.2) for the 1921 Da phosphopeptide found in fraction 8. The phosphorylation site was localized within the first 3 residues of the myosin V sequence 1648–64 but could not be conclusively determined. A small b_n ion series suggested that the major phosphorylation site was Ser1650 (see text). (D) Nano-ES (–) ion m/z 79 precursor scan of pooled fractions 7–9 showing that only a single peptide sequence is phosphorylated on myosin V. Two phosphopeptides with average masses of 1921.8 and 1982.6 were identified; however, the sequence of the 1982 Da phosphopeptide was determined by tandem MS to be the same as that of the 1921 Da phosphopeptide with a modification near the N terminus.

by nano-ES tandem MS. The spectrum for the peptide in fraction 8 is shown in Figure 5C. In each case, we were able to locate the phosphorylation site(s) within the first 3 amino acids (Thr¹⁶⁴⁸, Ser¹⁶⁴⁹, Ser¹⁶⁵⁰). Because of the scarce information contained in the low- m/z region of the spectrum, the site of phosphorylation could not be conclusively determined. Considering that the three phosphopeptides (all with the same sequence) elute in three distinct peaks, it is likely that they represent the same phosphopeptide phosphorylated on each of the first three residues. However, in the spectrum from fraction 8, the presence of a weak b_2 ion at m/z 189 containing nonphosphorylated Thr¹⁶⁴⁸ and Ser¹⁶⁴⁹ and a weak b_3 – b_{16} ion series, which all contain a phosphate group, suggest that the major phosphorylation site is Ser¹⁶⁵⁰.

To rule out the possibility that the MALDI analysis had missed additional phosphopeptides in any of the three fractions, we combined them and analyzed both the mitotic and interphase samples by nano-ES using a precursor ion scan of m/z 79. The pooled fractions from the mitotic MGT sample contained the expected 1921 Da phosphopeptide (Figure 5D) plus a second peak with $M_r = 1982.6$. Using nano-ESMS/MS we confirmed that the 1982.6 phosphopeptide has the same sequence as the 1921 Da phosphopeptide (1648–1664) and was modified near the N terminus. The cause of this mass difference was not further

investigated. No other phosphopeptides were detected, confirming that a single sequence on MGT was selectively phosphorylated by the mitotic extracts. The precise localization of the major site of phosphorylation was accomplished by mutagenesis and was determined to be Ser¹⁶⁵⁰. These data and the functional analysis of this phosphorylation are reported elsewhere.¹¹

CONCLUSIONS

In this report, we have described a modification of the multidimensional phosphopeptide mapping strategy described by us earlier.⁵ These modifications have improved the sensitivity of the method sufficiently to allow routine phosphopeptide analysis of gel-derived proteins. The mapping strategy uses LC/MS in the first dimension to identify phosphopeptide-containing HPLC fractions by monitoring for the presence of phosphate marker ions. In the second dimension, the molecular weight of phosphorylated peptides in the selected fractions is determined by precursor ion scanning. The exact site of phosphorylation is then determined by nanoelectrospray tandem MS. As previously reported, the sensitivity of the method was ~ 5 pmol,⁵ making it difficult to access phosphoproteins available in limited amounts and purified by SDS-PAGE.

The sensitivity of the previous instrumental setup was limited by the HPLC column diameter used in the first-dimension analysis. The use of 0.5-mm-i.d. columns represented a practical lower limit for collecting HPLC fractions while still maintaining sufficient flow into the conventional ES source of the mass spectrometer. In this work, we have shown that by incorporating a microionspray source that accommodates flow rates on the order of 200–400 nL/min into the MS, we are able to adopt capillary HPLC columns with HPLC flow rates of 4 μ L/min. With this flow rate, a 7:1 split after the column sends the required 500 nL/min to the MS while still providing a flow sufficient for fraction collection. The current configuration has yielded a practical sensitivity of 100–200 fmol for any given phosphopeptide, representing a sensitivity enhancement of at least 20-fold over the previous experimental configuration. Previously, Jedrzejewski and Lehmann²³ had adopted our original use of peptide marker ions for capillary column LC/MS. In a cleverly designed experiment, they took advantage of software control to switch a quadrupole MS between negative ion marker scans and positive ion full MS scans for phosphopeptide detection. Using an HPLC column of dimensions similar to ours, they also demonstrated phosphopeptide marker ion sensitivity of 200 fmol. However, since all of the flow from the column was sent to the MS, it was not possible to sequence any of the phosphopeptides detected. In addition, the extreme difficulty of identifying low stoichiometry phosphopeptides in the presence of much larger amounts of nonphosphorylated peptides is a severe limitation of any technique that relies upon full scan MS spectra for the task. This was commented upon by us previously.^{2,5}

The ability to further analyze each of the phosphopeptides or phosphopeptide-containing fractions individually is a major advantage of this technique over those that work from unseparated mixtures.^{8,24} For the second dimension analysis, we evaluated the ability of MALDI-PSD to identify phosphopeptides in the HPLC fractions and compared it to the use of nano-ES and precursor ion scanning. MALDI-PSD analysis is a rather simple, fast method that uses very little of the selected HPLC fraction ($\sim 1/20$). We found that in cases in which the composition of the fraction is sufficiently simple or the phosphorylation stoichiometry fairly high, the use of MALDI-PSD represents a useful approach. Furthermore, for those laboratories not equipped with a triple quadrupole instrument, it is a valid approach that deserves to be pursued. It would be useful to write an instrument control script to automate the acquisition and analysis of large numbers of PSD spectra per sample.

Precursor ion scanning, on the other hand, effectively analyzes every peptide signal in the sample and can selectively identify very small amounts of phosphopeptides in a sample, even in the presence of large amounts of nonphosphorylated peptides.^{2,5,24} It is a highly selective technique that in principle has sensitivity equal to MALDI-PSD. In practice, we generally use between one-fourth and one-half of each fraction for precursor ion scanning and sequencing. Thus, starting with a mixture containing ~ 200 fmol of phosphopeptides, we were able to isolate, identify, and sequence the phosphopeptides present in the sample.

Recently, Steen et al.²⁵ reported on a new method for detecting phosphotyrosine-containing peptides that utilizes the phosphoty-

rosine immonium ion found at m/z 216 in the positive ion mode. Utilizing the high-mass accuracy of quadrupole-TOF hybrid mass spectrometers, the m/z 216.043 ion can be detected with high selectivity and sensitivity without interference from other low-mass ions. Because the analysis is done in the positive ion mode, there is no need to adjust the pH of the sample or switch instrument polarity to perform MS/MS. This greatly facilitates peptide sequencing. Although the sensitivity of the method is slightly lower when compared to detection of m/z 79 by precursor scanning on a modern triple-quadrupole instrument,²⁶ it is specific for phosphotyrosine residues. Although accounting for only 0.05% of all phosphorylated residues, tyrosine phosphorylation nevertheless plays a crucial role in many signaling pathways. Unfortunately, this method is not able to detect phosphoserine- and phosphothreonine-containing peptides.

The enhancement in sensitivity provided to our multidimensional method by the new experimental setup makes it suitable for phosphorylation mapping of gel-separated phosphoproteins. It can detect serine, threonine, and tyrosine phosphorylation equally well where the amount of any given phosphopeptide is 100–200 fmol. In fact, the method is well-suited to multiply phosphorylated proteins because of the fractionation step employed in the first dimension. We have shown here the identification of 12 phosphopeptides from the protein kinase YAK1. These peptides represent serine, threonine, and tyrosine phosphorylation and correspond to 11 *in vivo* derived phosphorylation sites. This analysis was done from a single SDS-PAGE band from immunoprecipitated YAK1. Approximately 2 pmol of protein was loaded onto the gel, and we estimate, on the basis of the signal derived from the internal standard, that 200 fmol or less of each phosphopeptide was present. Not only does this sensitivity compare well with other high-sensitivity phosphorylation mapping studies,^{8,24,25} but it also clearly demonstrates the ability of this method to detect and identify multiple low-abundance or low-stoichiometry phosphorylation sites.

Determining which, if any, of the phosphorylation sites mapped on a protein are functionally significant usually involves mutagenesis of the phosphoacceptor sites, either individually or in combination, and then reassaying the proteins function. It would be convenient if there were a more expeditious way to evaluate the functional significance of multiple phosphorylation sites on a protein. The phosphate-selective m/z 79 trace provided by the marker ions in the first dimension LC/MS analysis produces a phosphorylation profile. Because of the generally good reproducibility of liquid chromatography, this phosphorylation profile can serve as a fingerprint for the phosphorylation state of the protein. Comparing the phosphorylation profiles for a given protein derived under two different conditions (for instance, activated and inactivated) would allow a semiquantitative measure of the phosphorylation stoichiometry at various sites. Those sites showing changes in utilization under a certain set of conditions can be said to be functionally significant for that set of conditions.

In this work, we have shown that the phosphopeptide response is sufficiently quantitative over 2 orders of magnitude to be able to detect a 100-fold change in phosphorylation for a single peptide. Furthermore, unlike ³²P-based 2D phosphopeptide mapping,¹ this

(23) Jedrzejewski, P. T.; Lehmann, W. D. *Anal. Chem.* **1997**, *69*, 294–301.

(24) Neubauer, G.; Mann, M. *Anal. Chem.* **1999**, *71*, 235–242.

(25) Steen, H.; Kuster, B.; Fernandez, M.; Pandey, A.; Mann, M. *Anal. Chem.* **2001**, *73*, 1440–1448.

(26) Steen, H.; Kuster, B.; Mann, M. *J. Mass Spectrom.* **2001**, *36*, 782–790.

method uses no radioactive labeling, and the analysis (apart from sample prep, which is the same in both cases) takes only ~20–30 min per sample. In the case of myosin-V, a single phosphorylation site from among several was identified as being responsible for cargo binding. This was accomplished by comparing the phosphorylation profiles of the protein after treatment with either interphase extract (cargo binding) or mitotic extract (no cargo binding). In fact, this example shows quite clearly that it may not be necessary to map all of the *in vivo* phosphorylation sites on a protein if it is possible to measure a protein's phosphorylation-dependent function. After examining the phosphorylation profiles of the functional and nonfunctional protein, only those phosphorylation sites that exhibit a change in stoichiometry need to be considered. On the other hand, where the only requirement of the phosphorylation profile is to monitor the levels of known phosphorylation sites under varying cellular conditions (like cell cycle changes) and no subsequent analysis was anticipated, sensitivity in the low femtomole range could be achieved by the use of even smaller diameter (50–75 μm) HPLC columns. It is important to note that this method does not measure absolute stoichiometry, but rather, measures a relative change. Whereas the myosin-V example reflected a dramatic change in phosphorylation stoichiometry at a single site, we have also recently shown that this approach can detect more subtle changes at multiple sites from *in vivo*-derived, SDS-purified proteins.²⁷

(27) Chen, S. L.; Huddleston, M. J.; Carr, S. A.; Annan, R. S.; Shou, W.; Deshaies, R. J. Proceedings of the 49th Conference on Mass Spectrometry and Allied Topics, Chicago, IL, 2001.

(28) Zhang, X.; Jin, Q. K.; Carr, S. A.; Annan, R. S. Proceedings of the 49th Conference on Mass Spectrometry and Allied Topics, Chicago, IL, 2001.

(29) Biemann, K. In *Methods in Enzymology*; McCloskey, J. A., Ed.; Academic Press: San Diego, New York, 1990; Vol. 193, Mass Spectrometry; pp 886–887.

In cases where a differentially phosphorylated peak in the phosphorylation profile contains more than one phosphopeptide, it will not be possible to determine which is responsible for the differential response. The irregular timing of collecting fractions and the variable response of samples in nano-ES also rules out the use of precursor scans for making a quantitative comparison of two different samples. A viable alternative in these cases is comparison of the peak ratio for the phosphorylated and non-phosphorylated peptides from the two samples measured in a positive ion LC/ESMS experiment.² Another alternative is the use differential of isotope labeling for measuring the site-specific, relative phosphorylation change between two samples. Recently, we introduced a novel isotope-labeling approach which uses N-terminal isotope-encoded tagging (NIT) for a more strict quantitation of both absolute phosphorylation stoichiometry as well as relative changes in phosphorylation at a specific site in response to cellular changes.²⁸ Each sample is labeled with a different isotope tag (d_0 or d_5), and the samples are mixed. In a single measurement, the relative phosphorylation for the two samples can be determined. The incorporation of the NIT chemistry into the multidimensional phosphopeptide mapping protocol will provide a powerful tool for studying phosphorylation-dependent biological processes.

ACKNOWLEDGMENT

The authors thank Drs. C. L. Creasy and S. Kassis for providing the YAK1 sample. V.I.G. and R.L.K. were supported by NIH grant GM-52111.

Received for review January 23, 2002. Accepted April 1, 2002.

AC025538X